ARTICLE IN PRESS

Short communication

Silicon photomultiplier (SPM) detection of low-level bioluminescence for the development of deployable whole-cell biosensors: Possibilities and limitations

Huaqing Li, Nicholas Lopes, Scott Moser, Gary Sayler, Steven Ripp*

The Center for Environmental Biotechnology and the Department of Microbiology, The University of Tennessee, Knoxville, TN 37996, USA

ABSTRACT

Whole-cell bacterial bioreporters await miniaturized photon counting modules with high sensitivity and robust compatible hardware to fulfill their promise of versatile, on-site biosensor functionality. In this study, we explore the photon counting readout properties of the silicon photomultiplier (SPM) with a thermoelectric cooler and the possibilities of detecting low-level bioluminescent signals. Detection performance was evaluated through a simulated LED light source and the bioluminescence produced by the genetically engineered *Pseudomonas fluorescens* bacterial bioreporter 5RL. Compared with the conventional photomultiplier tube (PMT), the results revealed that the cooled SPM exhibits a wider linear response to inducible substrate concentrations (salicylate) ranging from 250 to 5000 ppb. Although cooling of the SPM lowered dark count rates and improved the minimum detectable signal, and the application of a digital filter enhanced the signal-to-noise ratio, the detection of very low light signals is still limited and remains a challenge in the design of compact photon counting systems.

© 2012 Elsevier B.V. All rights reserved.

1. Introduction

Bioluminescence – the chemical generation of light within a living organism–is applied in a variety of bioanalytical methods due to its virtually absent background, high sensitivity, and wide dynamic range (Kaihara et al., 2009; Meighen, 1991; Roda et al., 2009). Unlike fluorescence which requires an external excitation light source (Close et al., 2009), bacterial bioluminescence, mediated by the *lux* gene cassette, is a form of chemiluminescence where the light-yielding reaction is derived from a naturally catalytic process directly within the cell and requires no exogenous substrates. Due to the absence of background bioluminescence in non-bioluminescent hosts, signal detection is only limited by the noise within the detector itself.

The integration of the *lux* gene cassette into bacterial, yeast, and human cells has created an inventory of whole-cell living bioreporters capable of sensing and responding to specific chemical, biological, and physical targets via the emission of light. Interfacing bioreporters with transducers to measure resulting light signals forms highly sensitive and autonomously deployable biosensors. However, to fully realize the potential of whole-cell biosensors, miniaturized, accurately calibrated, stand-alone photon counting systems or microluminometers are necessary. Because the bioluminescent reaction typically yields low light intensities, a highly

sensitive transducer interface is required. Effective and accurate photon counting methods using a photomultiplier tube (PMT) have been performed with bacterial bioreporters. Low dark counts in the PMT enable low threshold detection limits (Polyak et al., 2001), however, the high operation voltage (>1000 V), high cost, relatively large size, and as we demonstrate here, lack of a dynamic linear detection range, makes it unsuitable for compact designs of integrated biosensing systems.

Recently, the silicon photomultiplier (SPM), which is capable of lower light detection (Jackson, 2007), has been garnering interest for medical imaging, low-power X-ray imaging, optical diffusion tomography imaging, and neutron science (Bencardino and Eberhardt, 2009; Herbert et al., 2007). Except for its comparable gain and photon detection efficiency, the solid state SPM, which is compatible with standard complementary metal oxide-semiconductor (CMOS) technology, has numerous advantages over the PMT including small size, low bias voltage, insensitivity to magnetic fields, and immunity to damage from light overexposure (Buzhan et al., 2003; Dolgoshein et al., 2006; Pignatel, 2008; Stewart et al., 2008). These distinguishing properties make it possible to integrate the SPM sensing and processing units, allowing for rapid detection of small-volume samples at a low cost. Importantly, in the photon counting mode, the gain of a PMT in response to a single incident photon varies widely due to excess noise limiting its application, while the SPM detector has a uniform gain in response to single photons (Stewart et al., 2009). Recently, Daniel et al. (2008) demonstrated the detection of bacterial bioluminescence using an SPM at room temperature.

* Corresponding author. Tel.: +1 865 974 9605; fax: +1 865 974 8086.
  E-mail address: saripp@utk.edu (S. Ripp).

In this work, we explored the possibilities and limitations of detecting low-level bioluminescence using a cooled SPM. Initially, photon-counting performance was evaluated using a simulated light emitting diode (LED) source followed by direct detection of weak bioluminescence emission from the bacterial bioreporter *Pseudomonas fluorescens* 5RL.

2. Methods

2.1. Bioreporter growth and maintenance

P. fluorescens 5RL was the bacterial strain used for analytical testing. Strain 5RL harbors a plasmid-borne construct containing an insertion of the bioluminescent *luxCDABE* gene cassette from *Vibrio fischeri* located within a salicylate (*sal*) degradative operon (King et al., 1990). Upon exposure to salicylate (salicylic acid; CAS #69-72-7), strain 5RL self-generates inducible bioluminescence at intensities that are dose dependent upon salicylate concentration. Detection limits range from 50 parts-per-billion (ppb) to >5 parts-per-million with corresponding response times of 70–20 min, depending on the sensitivity of the transducer interface used (Nivens et al., 2004; Ripp and Sayler, 2005) with reproducibility and robustness demonstrated across experimental regimens ranging from ecological studies of microbial communities and rhizosphere interactions (Cook et al., 2006; de Weger et al., 1997; Ho et al., 2007; Johnston, 1996; Mogil'naya et al., 2005) to the monitoring of bacterial colonization of dental root-canals (Sedgley et al., 2004, 2005).

Strain 5RL was grown from $-80\,°C$ freezer stock on Luria-Bertani (LB) solid media containing tetracycline at $14\,mg/mL$ (Tc_{14}) to maintain plasmid selection with overnight incubation at room temperature. The next day, a single colony of 5RL cells was inoculated into 100 mL of LB plus Tc_{14} liquid media in a 250 mL Erlenmeyer flask and incubated for 16 h at room temperature with shaking at 140 rpm. Experiments commenced by adding 5 mL of this culture to 250 mL of minimal salts media (MSM) supplemented with Tc_{14}, 10 mL of a 20 g/L glucose stock, and 20 μL trace elements (Burlage et al., 1994) in a 500 mL Erlenmeyer flask coupled to a flow-through system consisting of a Masterflex pump (Cole-Parmer, Vernon Hills, IL, USA), Masterflex tubing, and an 8 cm × 1.5 cm ($\sim$20 mL volume) quartz flow cell interfaced with the light detection instrumentation (see Sections 2.2 and 2.3 for details).

2.2. Light detection instrumentation

Bioluminescence emanating from the *P. fluorescens* 5RL culture was detected in a flow cell interfaced in tandem with an SPM and a PMT. The SPM consisted of a SensL SPMmini 1035 × 08 module (SensL, Cork, Ireland) containing an array of 400 avalanche photodiodes (APDs) with individual cell dimensions of 50 μm × 50 μm providing a photosensitive area of 0.01 cm². An integrated Peltier cooler driving circuit provided cooling down to $-20\,°C$. The SPM was connected to a personal computer (PC) through a USB interface. The integration time and threshold level were user controlled via the PC. Data were sampled and further processed by a program composed in LabWindows/CVI (version 8.2, National Instruments) and outputted as photon counts per second (cps).

The PMT consisted of a compact H7467 series Hamamatsu photon counting head operating at room temperature with a photosensitive area of 0.5 cm² (Hamamatsu, Bridgewater, NJ, USA). An RS232 interface provided direct PC connection. Software for PMT control and data download (in cps) was custom developed in Visual Basic. The performance specifications of the SPM versus the PMT are listed in Supplementary Table S1.
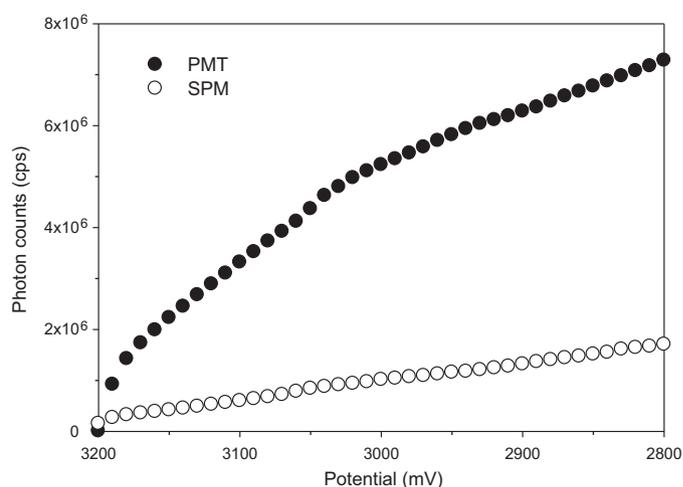

Fig. 1. Performance evaluations of the SPM ($\bigcirc$) and PMT ($\bullet$) photon counting detectors under simulated LED light exposure.

As even moderate light levels can saturate the SPM and high light levels can irreversibly damage the PMT, all experiments were performed in a light-tight housing that enclosed the detectors and the interfaced flow cells.

2.3. Format of the flow-through system

The culture of *P. fluorescens* 5RL cells in MSM plus supplements described in Section 2.1 was placed on a rotary shaker (140 rpm) at room temperature and pumped circuitously through sterile Masterflex Precision Norprene (A 60 G) tubing, through the flow cell, and back into the flask at a flow rate of 340 mL/min. The culture's optical density at 546 nm (OD_{546}) was monitored hourly until reaching 0.08 ($\sim$9 × 10^7 cells/mL (Nivens et al., 2004); established as time zero) whereupon salicylate was added to the flask at concentrations of 100, 250, 500, 1000, 2000, or 5000 ppb. A non-induced 0 ppb control was also run to establish background photon cps originating from the 5RL culture. Bioluminescence was then monitored over the next 3 h via the interfacing of the flow cell with both the SPM and PMT. This interface was formed by clamping the flow cell directly in front of the photosensitive areas of the SPM and PMT. True dark counts were determined by capping the photosensitive areas of each detector and acquiring photon cps within the light-tight enclosure with no 5RL culture present. All measurements were acquired over an integration time of 0.1 s with each measurement then averaged over every 10 s interval.

2.4. LED light source experiments

To initially evaluate performance of the SPM and PMT systems, a simulated LED light source was constructed using a Luxeon Star LXHL-MB1C power light source with a 3021 series driver module (LumiLeds, San Jose, CA, USA). The intensity of the LED was controlled with a potentiostat (CHI 604, CH Instruments, Austin, TX, USA) and the linearity and the stability of the attenuated LED output was characterized with an ultra-cooled $-80\,°C$ CCD IVIS Lumina imaging system (PerkinElmer, Waltham, MA, USA). Images were collected every 30 s in luminescence mode at 1 s integration times with light measurements recorded as photon cps using the integrated Living Image software package.

2.5. Statistical calculations

Experimental runs per each salicylate concentration were performed in triplicate, as were the LED light source experiments.
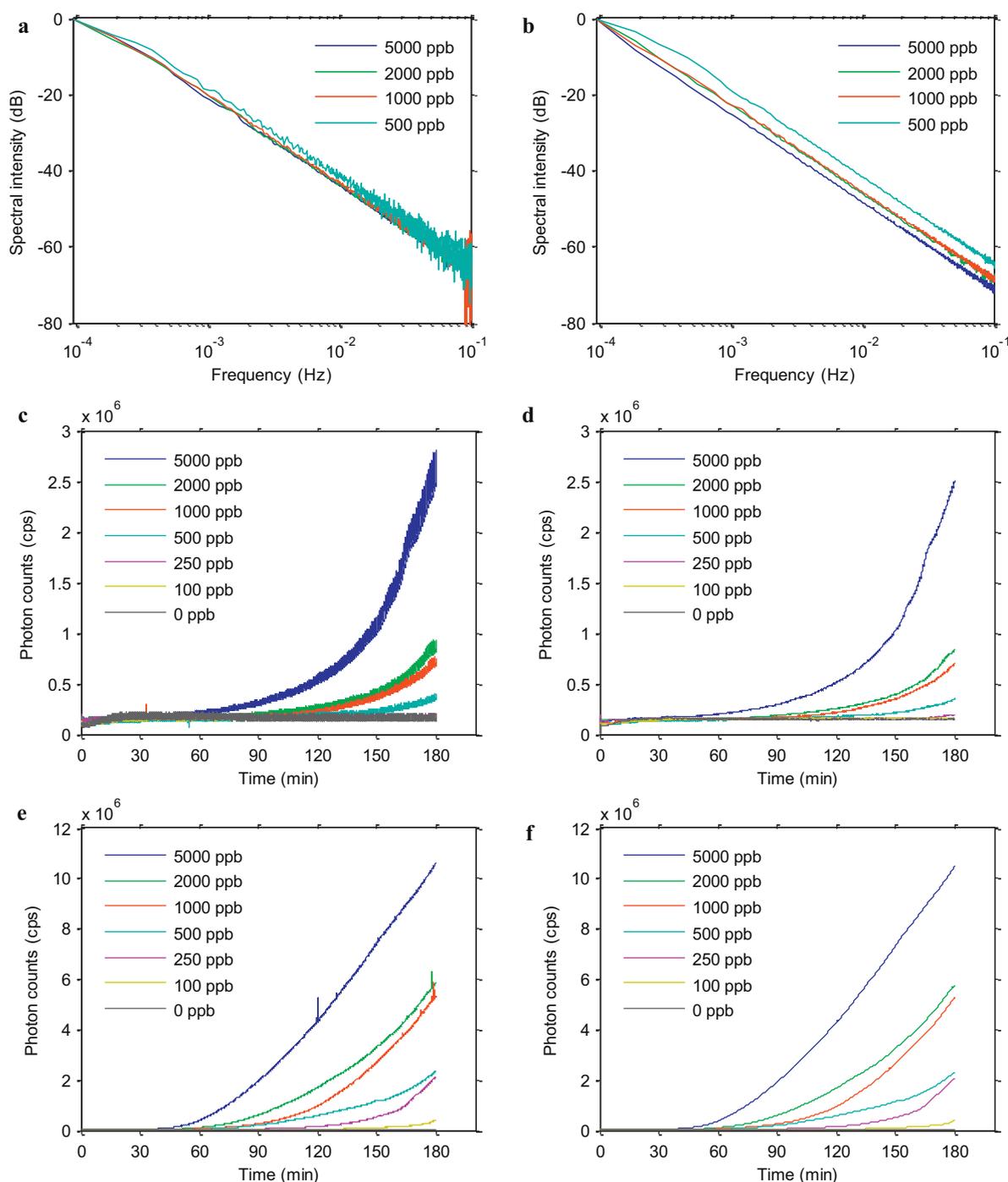
Fig. 2. The spectral intensity of bioluminescent emission from the *P. fluorescens* 5RL bioreporter under salicylate induction (500–5000 ppb) as measured by (a) the SPM and (b) the PMT, and the photon output (cps) under the full range of salicylate concentrations (100–5000 ppb; 0 ppb control) as recorded by (c) the SPM; (d) the SPM with digital low pass filtering; (e) the PMT; and (f) the PMT with digital low pass filtering.

Significant differences between each of the salicylate addition experimental runs were determined using the Student's *t*-test at $p < 0.02$. Error bars were calculated as the standard error of the mean.

3. Results and discussion

3.1. Linearity of the SPM and PMT response profiles against a simulated LED light source

The SPM and PMT photon counters were evaluated over a linear range of the LED light output. This required an initial validation of

the LED's linearity and stability, which, when characterized in an IVIS Lumina imaging system, demonstrated a light intensity that increased inversely to voltage over a range from 3400 to 2200 mV (Supplementary Fig. S1). Fig. 1 shows the light signals of the SPM and PMT modules analogously exposed to the voltage-controlled LED light with a scan rate of 1 mV/s. It is clear that the SPM photon counts are significantly less than that of the PMT under equivalent light exposures. One explanation for this is the smaller active area of the SPM. In fact, the PMT active area ($A = 0.5\,\text{cm}^2$) is 50 times larger than that of the SPM ($A = 0.01\,\text{cm}^2$). Importantly, however, the PMT displayed non-uniform linearity throughout its response profile and at higher light intensities (e.g., $>2 \times 10^6$ cps), detection

sensitivity progressively attenuated. Conversely, SPM photon counts were linear ($R^2 = 0.9978$) and demonstrated a uniform gain throughout the entire voltage scan. This suggests that the SPM, despite its small active area, possesses a more truly linear detection report of high light intensities relative to low light intensities.

3.2. Minimum detectable signal of the SPM

For a particular photon counting device, the minimum detectable signal (MDS) defined by the unity of the signal to noise ratio (SNR = 1) can be expressed by the equation (Daniel et al., 2008):

$$MDS = \frac{\sqrt{2 \cdot \bar{n}_d}}{\sqrt{\Delta T}}$$

And for a given detector with a quantum efficiency (η_D), the minimum detectable photons (P_{min}) can be expressed by:

$$p_{min} = \frac{\sqrt{2 \cdot \bar{n}_d}}{\eta_D \cdot A_D \cdot \sqrt{\Delta T}}$$

where $\bar{n}_d$ is the average rate of light counts or dark counts, ΔT is the integration time, and A_D is the effective area of the detector. Therefore, increasing the integration time or decreasing the dark counts improves the detectable signal level.

To decrease the dark count rate, a two-stage TEC Peltier cooler was built into the SPM module to reduce the temperature of the sensor to $-20\,°C$. The dark count rate of the cooled SPM was approximately 18×10^3 cps, which is a drastic reduction, by 15-fold, from the uncooled detector using similar technology with a dark count rate of 270×10^3 cps (Daniel et al., 2008). With this reduction, the MDS and P_{min} are decreased by 4-fold in principle. However, at the same integration time (e.g., 0.1 s), the P_{min} of the SPM normalized to its active area of 0.01 cm^2 (1.5×10^3 photons/s) is still much higher than that of the PMT normalized to its active area of 0.5 cm^2 (2.3×10^2 photons/s) due to the PMT's extremely low dark count rate and larger active area.

3.3. On-line flow-through detection of salicylate-induced bioluminescence

P. fluorescens 5RL was challenged with concentrations of salicylate ranging from 0 to 5000 ppb in a quartz flow-through cell interfaced on-line with the SPM and the PMT. The initial bioluminescent readout included a large amount of shot noise from the biological signal component and the dark count component of the photon detectors. Consequently, to minimize the noise and improve the detection sensitivity, a digital filter was applied to the signal readout. To find a matched filter, the effective bandwidth of the bioluminescence signal rate was calculated by converting the time-domain signals into frequency-domain waves using fast Fourier transform. Fig. 2 shows the normalized spectral intensity of bioluminescence for different concentrations of salicylate at different frequencies. The normalized intensity of the SPM signals is independent of the concentration (Fig. 2a), which agrees with the result from Daniel et al. (2008). Conversely, the spectral intensity of the PMT (Fig. 2b) shows a slight shift with concentration that may be due to the non-uniform amplification of the PMT. This result agrees with the LED simulation results (Fig. 1). Additionally, the intensity of the measured signals fluctuated due to the noise when light intensities were low. The SPM signal at 500 ppb salicylate, for example, was significantly influenced by noise, especially at high frequencies (e.g., >20 mHz).

In experiments applying the full range of salicylate concentrations from 0 to 5000 ppb both with and without integration of a
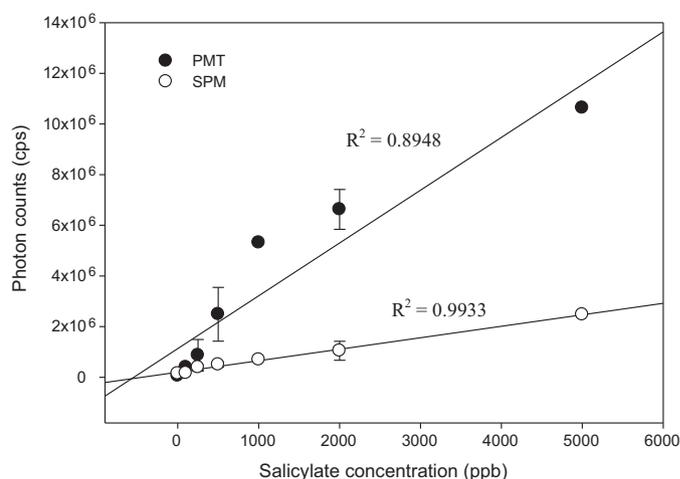

Fig. 3. Calibration curves for salicylate concentration versus the *P. fluorescens* 5RL bioluminescent response as measured by the SPM (○) and the PMT (●) at the maximally induced 3 h time point.

digital low pass filter with a cut-off frequency of 20 mHz, the measured signal intensities were shown to be concentration and time dependent with a positive correlation existing between intensity and each variable independently. Both photon detector modules consistently reported an increase in light output over the 3 h exposure period. The PMT, both with and without filtering, was more sensitive in its detection of low level bioluminescent signals, yet, as stated previously, this is principally due to its larger active area. For example, at the lowest tested 100 ppb concentration of salicylate, the SPM was unable to detect a significant bioluminescent response within the 3 h time course (Fig. 2c and d) whereas the PMT was capable of reporting a significant response at this concentration (Fig. 2e and f). It is important to note, however, that the smaller active area of the SPM, while not as effective in gathering low-level bioluminescence, is more practical for integration into deployable biosensor architectures.

Applying the digital low pass filter successfully improved SPM detection limits. Without filtering, the signal measured by the SPM at concentrations of 250 ppb salicylate and below was buried in the noise (Fig. 2c). After applying the digital low pass filter, the 250 ppb signal could be distinguished from the background (Fig. 2d). Applying the filter to the PMT did not result in improved detection limits but did yield considerably smoother curves due to an improvement in the signal-to-noise ratio.

Fig. 3 displays the calibration curve for salicylate concentration versus the *P. fluorescens* 5RL bioluminescent response as measured by the SPM and the PMT at the maximally induced 3 h time point. As with the LED simulation, the PMT demonstrates much higher sensitivity, however, the signal at concentrations above 500 ppb ($\sim 2.5 \times 10^6$ cps) abandoned a uniform linear relationship ($R^2 = 0.8948$). Conversely, the SPM was able to maintain a linear detection report ($R^2 = 0.9933$) throughout the entire range of salicylate concentrations from 250 to 5000 ppb. Therefore, the SPM has the ability to uniformly detect higher bioluminescence levels albeit with a lower sensitivity than the PMT. For developing sensitive, deployable biosensing modules, accurate calibration is mandatory and to this end the SPM is better suited with its uniform linear correlation between concentration and photon counts. One could, as has been done previously with studies employing the PMT for bacterial bioluminescent detection, perform a log transformation to linearize the non-linear model and simplify the relationship between the two variables (Polyak et al., 2001). However, interpretation of this fit becomes less meaningful due to the

now distorted standard deviations as the error effectively becomes ten-fold greater due to the log transformation.

4. Conclusions

The photon counting performance of an SPM and a conventional PMT were evaluated to explore the feasibility of low level bioluminescence detection. Cooling of the SPM improves the minimum detectable signal by dramatically decreasing the dark count rate. Although the sensitivity of the conventional PMT is higher due to its larger active area, detecting bioluminescence at salicylate concentrations down to 100 ppb, the more dynamic, solid-state SPM accurately produces a linear report over a much broader range of light intensities. Furthermore, by applying a low pass digital filter, the limit of detection of the SPM was improved down to 250 ppb due to the significant enhancement of the signal-to-noise ratio. For deployable biosensing, commercially available SPMs would benefit from dedicated on-board post-signal processing circuitry, however, this would detrimentally increase power consumption and size and introduce additional electronic noise. In past work, we have reported on an integrated circuit CMOS microluminometer that has evolved towards meeting some of the specific needs of deployable biosensing, including small size (1.5 mm × 1.5 mm), low power (<100 μW), and on-board signal processing (Islam et al., 2007; Vijayaraghavan et al., 2007). This so-called bioluminescent bioreporter integrated circuit, or BBIC, has been similarly tested with *P. fluorescens* 5RL in a flow-through format against salicylate challenges. Although the BBIC was capable of sensing bioluminescence from 5RL cultures induced with as little as 50–100 ppb salicylate, this detection limit was more so a result of the tuning of the BBIC to much longer integration times (1510 s) than those possible with an SPM or PMT. At this extended integration time, it was estimated that the BBIC could detect bioluminescence from approximately 5000 fully induced *P. fluorescens* 5RL cells (Bolton et al., 2002). With the integration time of the SPM set at its upper limit of 1 s, a calculated MDS can be approximated at 500 photons/s, which is three times below that of the BBIC's MDS of 1500 photons/s. Therefore, the SPM should theoretically detect as few as 1600 fully induced *P. fluorescens* 5RL cells, which suggests remarkable sensitivity and considerable potential towards biosensor applications coincident with a relatively small footprint and modest power demands.

Acknowledgements

Appendix A. Supplementary data

Supplementary data associated with this article can be found, in the online version, at doi:10.1016/j.bios.2012.01.008.

References

Bencardino, R., Eberhardt, J.E., 2009. IEEE Trans. Nucl. Sci. 56 (3), 1129–1134.
Bolton, E.K., Sayler, G.S., Nivens, D.E., Rochelle, J.M., Ripp, S., Simpson, M.L., 2002. Sens. Actuators B 85 (1–2), 179–185.
Burlage, R.S., Palumbo, A.V., Heitzer, A., Sayler, G., 1994. Appl. Biochem. Biotechnol. 45/6, 731–740.
Buzhan, P., Dolgoshein, B., Filatov, L., Ilyin, A., Kantzerov, V., Kaplin, V., Karakash, A., Kayumov, F., Klemin, S., Popova, E., Smirnov, S., 2003. Nucl. Instrum. Methods Phys. Res. Sect. A-Accel. Spectrom. Dect. Assoc. Equip. 504 (1–3), 48–52.
Close, D.M., Ripp, S., Sayler, G.S., 2009. Sensors 9 (11), 9147–9174.
Cook, K.L., Garland, J.L., Layton, A.C., Dionisi, H.M., Levine, L.H., Sayler, G.S., 2006. Microb. Ecol. 52 (4), 725–737.
Daniel, R., Almog, R., Ron, A., Belkin, S., Diamand, Y.S., 2008. Biosens. Bioelectron. 24 (4), 882–887.
de Weger, L.A., Kuiper, I., van der Bij, A.J., Lugtenberg, B.J.J., 1997. Antonie Van Leeuwenhoek 72 (4), 365–372.
Dolgoshein, B., Balagura, V., Buzhan, P., Danilov, M., Filatov, L., Garutti, E., Groll, M., Ilyin, A., Kantserov, V., Kaplin, V., Karakash, A., Kayumov, F., Klemin, S., Korbel, V., Meyer, H., Mizuk, R., Morgunov, V., Novikov, E., Pakhlov, P., Popova, E., Rusinov, V., Sefkow, F., Tarkovsky, E., Tikhomirov, I., 2006. Nucl. Instrum. Methods Phys. Res. Sect. A-Accel. Spectrom. Dect. Assoc. Equip. 563 (2),368–376.
Herbert, D.J., Moehrs, S., D'Ascenzo, N., Belcari, N., Del Guerra, A., Morsani, F., Saveliev, V., 2007. Nucl. Instrum. Methods Phys. Res. Sect. A-Accel. Spectrom. Dect. Assoc. Equip. 573 (1–2), 84–87.
Ho, C.H., Applegate, B., Banks, M.K., 2007. Int. J. Phytoremediation 9 (1–3), 107–114.
Islam, S.K., Vijayaraghavn, R., Zhang, M., Ripp, S., Caylor, S., Weathers, B., Moser, S., Terry, S., Blalock, B., Sayler, G.S., 2007. IEEE Trans. 54 (1), 89–98.
Jackson, C., 2007. Photon. Spect. 41 (12), 64–68.
Johnston, W.H., 1996. Fate of *Pseudomonas fluorescens* 5RL and its reporter plasmid for naphthalene biodegradation in soil environments. Center for Environmental Biotechnology. Master's Thesis, The University of Tennessee, Knoxville.
Kaihara, A., Sunami, A., Kurokawa, J., Furukawa, T., 2009. J. Am. Chem. Soc. 131 (12), 4188–4189.
King, J.M.H., DiGrazia, P.M., Applegate, B., Burlage, R., Sanseverino, J., Dunbar, P., Larimer, F., Sayler, G.S., 1990. Science 249, 778–781.
Meighen, E.A., 1991. Microbiol. Rev. 55, 123–142.
Mogil'naya, O.A., Krivomazova, E.S., Kargatova, T.V., Lobova, T.I., Popova, L.Y., 2005. Appl. Biochem. Microbiol. 41 (1), 63–68.
Nivens, D.E., McKnight, T.E., Moser, S.A., Osbourn, S.J., Simpson, M.L., Sayler, G.S., 2004. J. Appl. Microbiol. 96 (1), 33–46.
Pignatel, G.U., 2008. Inf. Midem-J. Microelectron. Electron. Compon. Mater. 38 (4), 225–236.
Polyak, B., Bassis, E., Novodvorets, A., Belkin, S., Marks, R.S., 2001. Sens. Actuator B-Chem. 74 (1–3), 18–26.
Ripp, S., Sayler, G.S., 2005. In: Osborn, M., Smith, C.J. (Eds.), Molecular Microbial Ecology. Taylor & Francis Group, New York, NY, pp. 321–344.
Roda, A., Guardigli, M., Michelini, E., Mirasoli, M., 2009. Trac-Trends Anal Chem. 28 (3), 307–322.
Sedgley, C., Applegate, B., Nagel, A., Hall, D., 2004. J. Endod. 30 (12), 893–898.
Sedgley, C.M., Nagel, A.C., Hall, D., Applegate, B., 2005. Int. Endod. J. 38 (2), 97–104.
Stewart, A.G., Saveliev, V., Bellis, S.J., Herbert, D.J., Hughes, P.J., Jackson, J.C., 2008. IEEE J. Quantum Electron. 44 (1–2), 157–164.
Stewart, A.G., Wall, L., Jackson, J.C., 2009. J. Mod. Opt. 56 (2–3), 240–252.
Vijayaraghavan, R., Islam, S.K., Zhang, M., Ripp, S., Caylor, S., Bull, N.D., Moser, S., Terry, S.C., Blalock, B.J., Sayler, G.S., 2007. Sens. Actuator B-Chem. 123 (2), 922–928.